ACCUMULATION OF HIGH INTENSITY BEAM AND FIRST OBSERVATIONS OF INSTABILITIES IN THE SNS ACCUMULATOR RING

V. Danilov, S. Cousineau, A. Aleksandrov, S. Assadi, W. Blokland, C. Deibele. S. Henderson, J. Holmes, M. Plum, A. Shishlo, SNS, ORNL, Oak Ridge, TN 37830, USA

Abstract

The Spallation Neutron Source storage ring, designed to accumulate up to 1.5e14 protons per pulse, was commissioned in January of 2006. During the run, over 1.e14 protons were accumulated in the ring in the natural chromaticity state without any sign of instabilities. The first beam instabilities were observed for a high intensity coasting beam with zero chromaticity. Preliminary analysis of data indicates instabilities related to extraction kicker impedances, resistive wall impedances, and electron-proton instability. Here we review the background theory and design philosophy of the ring, as it relates to instabilities, and compare the pre-commissioning predictions with the experimental measurements.

INTRODUCTION

The design philosophy of the Spallation Neutron Source (SNS) accumulator ring was centered around creating a lattice with minimal loss [1]. The first instability estimations (see, e.g., [2]) showed that electron cloud build-up might pose a risk for high current accumulation in the SNS ring. At the same time, experiments at the Proton Storage Ring (PSR) in Los Alamos demonstrated a promising reduction of the electron density in a chamber piece coated with a low secondary electron emission Titanium Nitrate (TiN) material (see [3] and references therein). This led to the decision to coat every piece of the SNS vacuum chamber with TiN. In addition, the ring was equipped with an electron collector near the stripping foil and reserved space for solenoidal magnets to reduce electron buildup in high loss regions [4]. Compared with predecessor machines, these are all new e-p mitigating features.

The next instability concern arose when the extraction kicker transverse impedance was measured (the first results were published later in [5]). The first estimations and simulations [6] showed that this impedance could generate an instability for high current ring operations, as well as create halo and beam loss (see the associated physics in, e.g. [7]). The extraction kicker was thus redesigned, and detailed measurements of the new kicker configuration indicated a successful reduction of the impedance (see, e.g., [8] and references therein), to well below the beam instability limits for nominal operating conditions.

In addition to the preventative measures for the e-p and extraction kicker instabilities listed above, space in the ring was also reserved for the possible installation of a broadband feedback system, if needed [9].

The third important instability issue is related to the injection kicker coating. The kicker has a ceramic vacuum chamber with a metallic coating which prevents the high frequency electromagnetic beam field from penetrating and affecting the kicker electronics. A very thin coating has a high resistivity, and produces a large longitudinal and transverse impedance at low frequencies [10]. It was found that this impedance, along with the resistive wall impedance of the remainder of the machine, can generate a closed orbit instability [11] (not investigated in this work). Fortunately, for the present choice of ring parameters, this impedance doesn't pose any threat for operations. But, the related instabilities can be observed if one switches from present ring working point (Q_x=6.23, Q_y=6.2) to a new one below the integer resonance.

The next section presents the details of the SNS ring relevant to high intensity operations, and an approach to estimate the transverse impedance from the instability data. The subsequent sections present the data and instability analysis, and the conclusions.

RING CONDITIONS AND HIGH INTENSITY BEAM PARAMETERS

The SNS Ring was successfully commissioned at the end of 2005 [12]. After commissioning, several beam runs were dedicated to high intensity studies. The experiments for the nominal working point (Q_x=6.23, Q_y=6.2) and natural chromaticity with measured values (ξ_x= -8.2, ξ_y= -7.2) showed no signs of instability in bunched beam mode. In this configuration, a bunched beam of 5.6×10^{13} protons was extracted from the ring with low loss. Further increase in intensity was stalled by beam loading effects on the ring RF system that led to substantial longitudinal beam distortion and a sharp increase of beam loss during extraction. Therefore, the instability studies continued without extraction for a coasting beam. Furthermore, to facilitate the investigation of impedances, the chromaticity was corrected to near zero; the measured residual values were around 0.1, i.e., reduced by almost two orders of magnitude compared to the natural ones. The energy spread from the linac was measured to be approximately 0.8 MeV for a 931 MeV beam.

For this energy spread and zero chromaticity, instabilities grew starting from 2×10^{13} protons in the ring.

Our approach for estimating the impedance was to go as high as possible in intensity and to measure the growth time for the observed instability. All impedances were obtained using the formula from [7]:

$$\mathrm{Re}(Z) = \frac{2\gamma\beta^2 E_0}{\tau \beta_{twiss} I}, \qquad (1)$$

where γ,β are relativistic parameters, τ is the growth time in turns, β_{twiss} is the beta-function at the impedance point (taken in most cases as the average over the ring), and I is the coasting beam current. The advantage of this approach for the impedance measurement with the beam, contrary to threshold- based estimations, is that it doesn't depend on the beam distribution when the instability is far above the threshold, as in our case.

FIRST INSTABILITIES OBSERVATION

Experimental Setup

Instability data was taken during three separate dedicated beam runs. In each of these runs, the machine was set up with off-nominal conditions conducive to instabilities. All of the instability runs were conducted with a coasting beam and no extraction from the ring; the beam was stored for tens of thousands of turns, and finally lost to the collimation system. In order to probe the instability parameter space, the following parameters were varied independently: Beam intensity, lattice tune, chromaticity, and RF cavity configuration (shorted or open gaps). The data for the RF state dependence has not yet been analyzed and therefore is not discussed in this paper.

For each beam pulse, data for the entire beam storage was recorded on a zero dispersion region BPM hooked up to an oscilloscope, with sampling rates in the range of 2-4 ns. For the accumulator ring revolution frequency of approximately 1 MHz, this allows for high resolution measurements over a large frequency range. A plot of the BPM scope trace for one of the first instabilities observed is shown in Fig. 1 below. The blue and yellow traces show the vertical and horizontal signals, respectively. The sharp spike at the end was identified as high frequency e-P instability, triggered by the beam loss from a low frequency, extraction kicker instability (this will be discussed more in a following section).

Extraction Kicker Instability

During the first beam instability run, an instability with frequency 6 MHz was observed for a zero chromaticity lattice with nominal lattice tunes of (Q_x=6.23, Q_y=6.2) The observed instability frequency of 6 MHz is a close match to the frequency associated with the peak of the lab-measured extraction kicker impedance [8]. Although in the lab-measurement the impedance had a dominant vertical component, experimentally we observe the instability in both directions, with a the vertical oscillation amplitude about a factor of three larger than the horizontal. We relate this behavior to the coupling resonance, and plan to confirm this theory in future experiments by tuning the lattice away from the resonance.

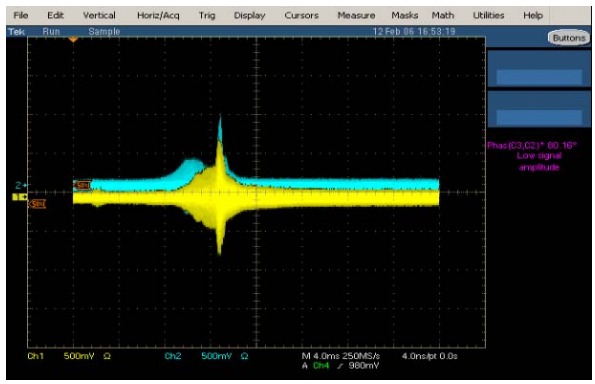

Figure 1: BPM traces of beam instability in the SNS accumulator ring. This particular data set exhibited two different types of instabilities. The full horizontal scale is about 20 ms.

Extraction Kicker Instability

During the first beam instability run, an instability with frequency 6 MHz was observed for a zero chromaticity lattice with nominal lattice tunes of (Q_x=6.23, Q_y=6.2) The observed instability frequency of 6 MHz is a close match to the frequency associated with the peak of the lab-measured extraction kicker impedance [8]. Although in the lab-measurement the impedance had a dominant vertical component, experimentally we observe the instability in both directions, with a the vertical oscillation amplitude about a factor of three larger than the horizontal. We relate this behavior to the coupling resonance, and plan to confirm this theory in future experiments by tuning the lattice away from the resonance.

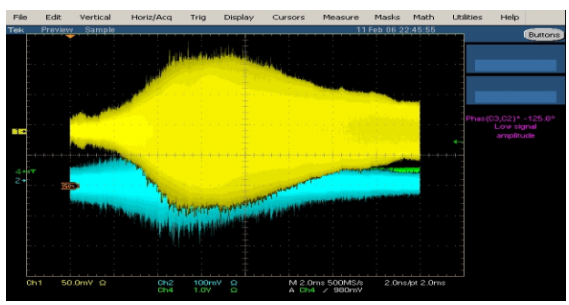

Figure 2: Scope trace of the impedance kicker instability for a 12 μC beam. The yellow trace is the horizontal data, and the blue is the vertical data.

A beam intensity scan showed that the instability is first present at around 3 μC. Even at the highest beam intensity observed, 12μC, the instability is slow and occurs over nearly a thousand turns. A BPM scope trace of the 12 μC beam instability is shown in Fig. 2, and a

waterfall plot of the turn-by-turn frequency spectrum, showing the dominant 6 MHz harmonic, is shown in Fig. 3.

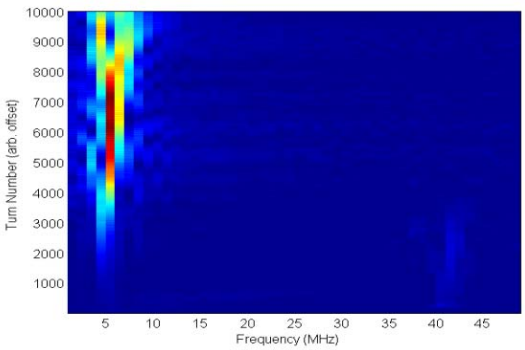

Figure 3: Turn-by-turn waterfall plot of the frequency spectrum of the instability shown in Fig. 2. The peak frequency of the instability is 6 MHz. The y-axis zero point indicates the beginning of the instability, not the point of injection into the ring.

The evolution of the 6 MHz harmonic can be used to calculate the impedance from Equation (1). Fig. 4 below shows the logarithm of the harmonic amplitude plotted versus turn number, from which the linear growth portion is used to estimate the growth time, τ. The impedance is found to be 28 kΩ/m, which is in close agreement with the predicted value of 22 - 30 kΩ/m.

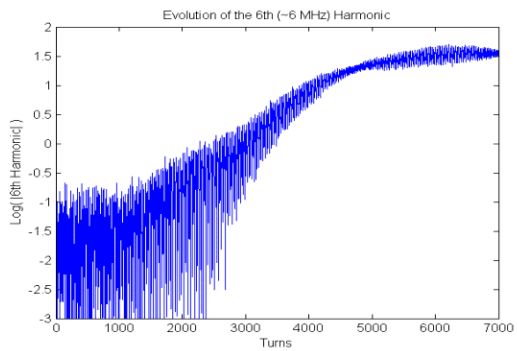

Figure 4: Turn-by-turn evolution of the 6 MHz harmonic amplitude.

Electron Proton Instability

During the second instability run we observed a fast, high frequency instability, which we associate with an electron-proton instability. Fig. 5 below shows waterfall plots of the frequency spectrum of the instability for three different beam intensities: 4 µC, 8 µC, and 16 µC.

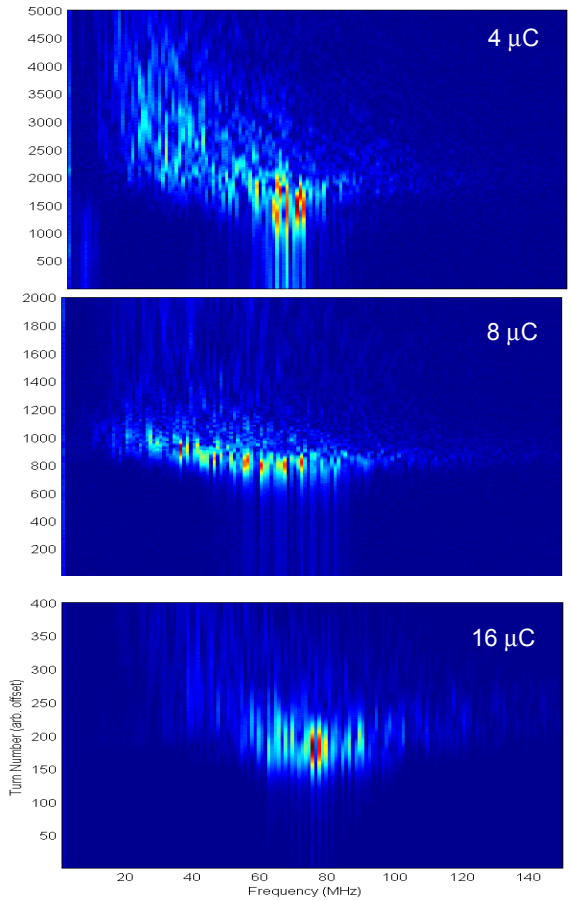

Figure 5: Turn-by-turn waterfall plots of the frequency spectrum of the instability for 3 different beam intensities, 4 µC (top), 8 µC (middle), and 16 µC.

The instability was studied by varying the beam intensity, the lattice tune, and the RF configuration. The RF tuning occurred during the last instability run, when we had higher beam losses and non-shorted RF gaps, which produced longitudinal bunching through beam-induced excitement of the cavities. As shown in Fig. 5 above, at lower beam intensities, the frequency peak of the instability is broader and lower, with a central peak of 60 MHz, and at the highest beam intensity, the frequency spread is smaller, with a more well-defined peak of 78 MHz. The frequencies are close to what we expect based on analytic calculations.

The instability occurs first and more strongly in the vertical plane. However, an interesting observation is that there appears to be coupling between the two transverse planes. The vertical instability induces a weaker instability of the same frequency in the horizontal plane. Additionally, the frequency content of the horizontal plane shows not only a peak at the horizontal lattice tune, but also a smaller peak at the vertical lattice tune. The frequency spectrum at the peak of the instability is shown in Fig. 6 below. Note the presence of both the horizontal fractional tune, Q_x=6.23, and the vertical tune, Q_y=6.20 .

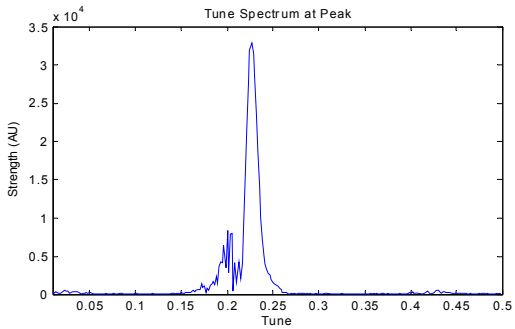

Figure 6: Frequency spectrum of the horizontal plane during the peak of the e-p instability.

Because the nominal operation lattice tunes for the ring, (Q_x=6.23, Q_y=6.2) are close to the coupling resonance, the lattice was retuned to a split tune of (Q_x=6.24, Q_y=6.16). This had little effect on the instability, which decreased only slightly in strength for the split-tune configuration.

In the data sets where it appears, the electron-proton instability often the only instability visible. This may be due to the BPM gains being adjusted for a strong instability, which would have the effect of dropping weaker instabilities into the noise level. However, a small handful of data sets showed the existence of more than one instability. In one particular data set, both the extraction kicker instability and the electron-proton instability are present in the horizontal plane of an 8 μC beam. The BPM trace of the instability is shown in Fig. 1. The extraction kicker instability was found near the usual frequency of 6 MHz, and was followed 2000 turns later by the electron-proton instability, which was shifted to a lower than typical frequency of 20 MHz. In this case, the fast instability probably occurred due to beam loss from the first, low frequency instability. Fig. 7 below shows the frequency spectrum of the two instabilities.

Although the electron-proton instability can not be associated with the impedance of an element of hardware, we can nonetheless apply Equation (1) for the instability and derive the effective impedance of the instability. This calculation was performed for the 8 μC beam case and again for the 16 μC case, and yielded impedances of 168 kΩ/m, and 1.9 MΩ/m, respectively. Thus, the e-p impedance is much larger than the conventional impedances, and depends on the beam current.

Resistive Wall Instability

In the last high intensity run, the lattice was tuned to the below integer values of (Q_x=5.81, Q_y =5.80), where the slow mode instability then occurs at a frequency of 200 kHz, where the resistive wall and injection kicker coating impedances are large. The analysis of the data from this run is still underway, and the results listed below are preliminary.

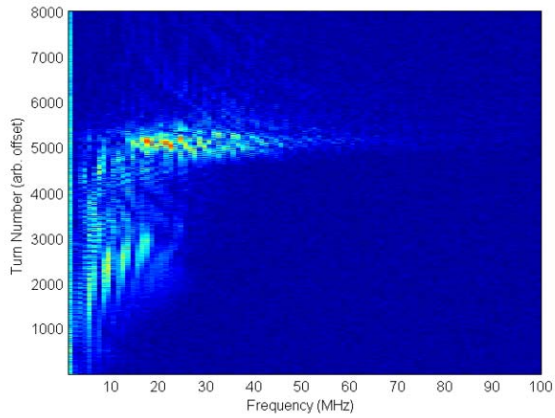

Figure 7: Frequency spectrum, showing the presence of both slow and fast instability (extraction kicker and e-p instability).

Analysis of the BPM data for a 6 μC beam showed a sharp, isolated peak at 191 KHZ, very close to the predicted resistive wall instability. The frequency spectrum of the data is shown in Fig. 8. In our preliminary assessment, we attribute this peak to the resistive wall instability, resulting from the total ring resistive wall impedance; more data will be necessary to confirm our theory. After approximate scaling for BPM sensitivity effects at lower frequencies, the oscillation amplitude of the instability is at least a factor of three weaker than the e-P instability, which is visible in the same data set.

Figure 9 shows the evolution of the 191 MHz harmonic during the instability. The impedance of the instability was estimated using Equation (1) to be 34 kΩ/m. The real part of the impedance value estimated for the injection kicker is around 25 kΩ/m, and the resistive wall real part is around 14 kΩ/m. The uncertainty in the calculated impedance values is about 50%, stemming from an uncertainty of the injection chamber thickness and the non uniformity of the vacuum chamber geometry.

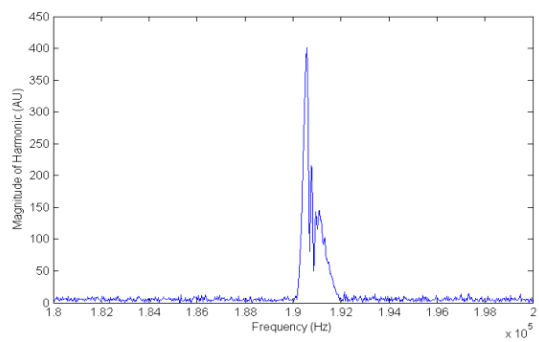

Figure 8: Frequency spectrum of the resistive wall instability.

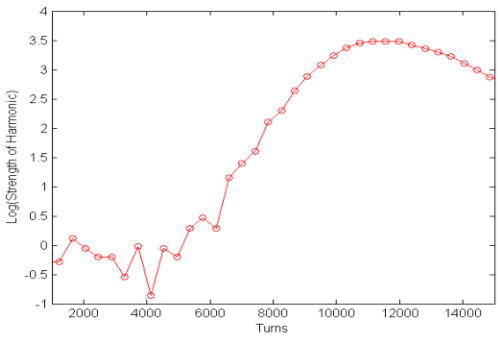

Figure 9: Evolution of 191 kHz harmonic amplitude. The estimated growth time is about 1300 turns.

CONCLUSIONS

By intentionally running the SNS accumulator ring in a state which is conducive to instabilities, three types of transverse instabilities were observed: extraction kicker instability, electron-proton instability, and resistive wall instability. Both the extraction kicker impedance and the resistive wall impedance derived from the data and Equation (1) are in good agreement with the predicted, calculated impedance.

Of the three instabilities, first observations indicated that the electron-proton instability is the fastest and the strongest. Coupling between the horizontal and vertical planes is observed for this instability. It is possible, but yet unknown, if this instability is generally triggered by one of the other two instabilities, or by an independent effect.

ACKNOWLEDGMENTS

Research on the Spallation Neutron Source is sponsored by the Division of Materials Science, U.S. Department of Energy, under contract number DE-AC05-96OR22464 with UT-Battelle Corporation for Oak Ridge National Laboratory.

REFERENCES

[1] J. Wei, *et al*, "Low-loss design for the high intensity accumulator ring of the Spallation Neutron Source", Phys. Rev. ST Accel. Beams 3, 080101 (2000)

[2] V. Danilov *et al*, ICFA Workshop on Instabilities of High Intensity Hadron Beams in Rings, Upton, New York, June 1999

[3] B. Macek, *et al*, "Status of experimental studies of the electron cloud at the Los Alamos Proton Storage Ring, PAC 2003, Portland, May 2003

[4] L.F. Wang, *et al* , "Mechanism of electron cloud clearing in the accumulator ring of the Spallation neutron Source", Phys. Rev. ST Accel. Beams v 7, 034401 (2004), and L.F. Wang, *et al*, "Stripped electron collection at the Spallation Neutron Source", Phys. Rev. ST Accel. Beams, v 8, 094201 (2005)

[5] J. G. Wang and S. Y. Zhang, "Coupling Impedance Measurements of a Model Fast Extraction Kicker Magnet for the SNS Accumulator Ring", *Nucl. Instr. & Meth. in Phys. Res. A* **522**, pp. 178-189, April 2004.

[6] V. Danilov, *et al*, "Transverse Impedance Implementation in ORBIT", PAC 2001, Chicago, USA, June, 2001 A. Fedotov, *et al*, "Exploring Transverse Beam Stability in the SNS in presence of space charge", EPAC02, Paris, June 2002.

[7] V. Danilov and J. Holmes, "Halo and RMS Beam Growth due to Transverse Impedance", ICFA Workshop on Halo in Proton Accelerators, Shelter Island, NY 2002

[8] H. Hahn, "Impedance measurements of the Spallation Neutron Source extraction kicker system", Phys. Rev. ST Accel. Beams **7**, 103501 (2004)

[9] S. Henderson, V. Danilov, ASAC presentations, Oak Ridge, TN, September, 2004

[10] V. Danilov, S. Henderson, A. Burov, V. Lebedev, "An improved impedance model of metallic coating", EPAC 2002, Paris (2002)

[11] V. Danilov, *et al*, "Closed orbit instability", Physical Review Special Topics – Accelerators and Beams **4**, (2001), 120101.

[12] S. Henderson, "Recent commissioning results of SNS", these proceedings.